Identification of microRNAs regulated by miR-168a-mediated Argonaute1 in response to potassium deficiency stress in tomatoes

Xin Liu[1], Chunchang Tan[1], Xin Cheng[1], Xiaoming Zhao[1], TianLai Li[1], and Jing Jiang[1]

[1]Shenyang Agricultural University

May 5, 2020

Abstract

Potassium (K+) is an essential macronutrient involved in regulating plant growth and development. K+ homeostasis in plant cells is modulated to facilitate plant adaptation to K+-deficiency stress. Argonaute1 (AGO1) interacts with miR-168a to modulate the small RNA regulatory pathway in tomatoes. However, the roles of AGO1 and miR-168a in modulating K+ deficiency stress in tomatoes have not been elucidated. Accordingly, in this study, we examined the interactions between AGO1 and miR-168a in mediating low-K+ stress in tomato plants. SlmiR-168a and its target SlAGO1 were differentially expressed between low-K+ tolerant JZ34 and low-K+ sensitive JZ18 tomato plants. Transgenic tomato plants constitutively expressing SlmiR-168a and rSlAGO1 (SlmiR-168a-resistant) showed different root hair development, leaf phenotypes, and K+ contents in roots under K+-deficiency stress. Sequencing analyses showed that 446 microRNAs (miRNAs) and 541 miRNAs were differentially expressed in 35S:SlmiR-168a compared with wild-type (WT) tomatoes and in 35S:rSlAGO1 compared with WT tomatoes, respectively. Twelve miRNA/mRNA pairs were identified, and the root growth and cytokinin (CTK)/abscisic acid (ABA) pathways were shown to be involved in SlmiR-168a-mediated SlAGO1 regulatory network in response to K+-deficiency stress. Thus, SlAGO1 regulated by SlmiR-168a may influence downstream miRNA pathways in response to low-K+ stress though modulating root growth and CTK/ABA pathways.

Introduction

Potassium (K^+) is an essential element with various functions in many physiological processes, such as osmoregulation, photosynthesis, enzyme activation, membrane potential maintenance, and ion homeostasis (Clarkson & Hanson, 1980). These functions rely on high and relatively stable concentrations of K^+ in cellular compartments and K^+ movement between different compartments, cells, and tissues. Accordingly, K^+ must by readily transported or regulated. K^+ exists in plants as an ion and is highly mobile. In the soil, $K^+$is taken up by plants through root absorption. The K^+concentration differs among subcellular regions of plant cells; for example, the concentration of K^+ in the cytoplasm is generally maintained at approximately 100 mM, whereas that in the vacuoles varies to facilitate the storage of K^+ in the cell (Besford & Maw, 1975). Compared with the high concentration of K^+ in cells, the concentration of K^+in the soil is very low. Moreover, because the roots of the plant are in direct contact with the soil, the K^+ deficiency signal is first perceived by root cells, particularly root epidermal cells and root hair cells (Song et al. 2017). Plants respond to low K^+ concentrations by altering root growth and root configuration, such as inhibiting primary roots and stimulating root hair elongation (Cao et al. 1993). In plants, low K^+signal transduction causes a downstream response, ultimately promoting the adaptation of the response to K^+ deficiency in plants (Han et al. 2018). Notably, K^+ deficiency can activate K^+ uptake through plant roots by regulating the activity of K^+ transporters (Gierth & Maser, 2007).

Some signalling molecules, including reactive oxygen species (ROS), Ca^{2+}, plant hormones, and microRNAs (miRNAs) are involved in plant responses to low K^+ stress (Wang & Wu, 2017). In *Arabidopsis* , K^+ deficiency induces the production of ROS and the expression of the NADPH oxidase gene *RHD2* and the

peroxidation enzyme gene *RCI3* (Shin & Schachtman, 2004). In addition to ROS, Ca^{2+} also acts as a low K^+ response signal. Recently, the Ca^{2+} reporter YC3.6 was observed to be induced by low K^+ (Behera et al. 2017). Additionally, previous studies have revealed that some phytohormones (ethylene, auxin, cytokinin [CTK], and jasmonic acid) are involved in signal transduction of plant responses to K^+-deficiency stress. In *Arabidopsis thaliana* , low K^+-induced ethylene signalling regulates K^+ transporter 5 (*AtHAK5*) transcription and root growth through modulation of ROS signalling (Schachtman, 2015). Moreover, by regulating the localisation of auxin transporter AtPIN1, the K^+ transporter AtTRH1/AtKUP4 plays important roles in the regulation of K^+-dependent root architecture in *Arabidopsis thaliana* (Rigas et al. 2013; Dolan, 2013). Low-K^+stress downregulated CTK levels, which stimulates ROS accumulation, root hair growth, and AtHAK5 expression (Nam et al. 2012). The expression of the K^+ transporter gene OsCHX14, which is involved in K^+ homeostasis in rice flower, is regulated by jasmonic acid signalling (Chen et al. 2016). Taken together, these phytohormone signalling pathways may constitute a regulatory network and synergistically control root architecture and K^+transporter expression under low-K^+ conditions.

Compared with miRNA studies of other nutrient (e.g., N, P, S, and Cu) deficiencies, few reports have evaluated K^+ deficiency (Hu et al. 2015; Kulcheski et al. 2015). A recent study showed that*miR-399* is involved in responses to multiple nutrient deficiencies in rice (*Oryza sativa*) by regulating the absorption of multiple nutrient (Hu et al. 2015). In *O. sativa* ,*miR-399* is also induced by low-K^+ stress and represses its downstream target listerin E3 ubiquitin protein ligase 1/PHO2. In plants, after RNase III Dicer-like 1 cutting, the miRNA strand of the miRNA:miRNA* duplex is loaded into an Argonaute (AGO) protein, which has a single-stranded RNA-binding PAZ domain and an RNaseH-like PIWI domain to catalyses mRNA cleavage or translational repression (Reinhart et al. 2002; Tomari & Zamore, 2005). miRNAs are loaded into AGO1, which acts as an RNA slicer (Qi et al. 2005). Among the 10 plant *AGO* mRNA homologs, only *AGO1* has extensive complementary to *miR-168* or any other known miRNAs, suggesting that *AGO1* may be the only member of the AGO family to be regulated by miRNAs (Vaucheret et al. 2004). In *Arabidopsis* , fine-tuned post-transcriptional regulation of *miR-168* and*AGO1* levels maintains the expression balance of other miRNAs, which, together with AGO1, control the mRNA expression levels of miRNA targets (Vaucheret et al. 2006).

In this study, we aimed to evaluate the balance between *miR-168a*and *AGO1* expression in response to K^+deficiency stress in *Solanum lycopersicum* . We also verified influence of *SlmiR-168a* -dependent *SlAGO1* on plant growth under K^+-deficiency stress and used miRNA-Seq and mRNA-Seq results to assess the regulatory mechanism of*SlmiR-168a* -mediated *SlAGO1* in the response to K^+ deficiency.

Materials and Methods

Plant materials and growth conditions

Seedlings of two tomato genotypes (JZ34 [low K^+tolerant] and JZ18 [low K^+ sensitive]) (Zhao et al. 2019) were grown under standard greenhouse conditions at 26/18 (day/night) with a photoperiod of 16 h light/8 h dark. Seedlings at the vegetative growing stage (25 days) were cleaned with water, washed three times with distilled water, and transferred to a pot (50 cm length, 30 cm width, 10 cm height) containing 12 L nutrient solution composed of 1.5 mM $Ca(NO_3)^2 \cdot 4H_2O$, 4 mM KNO_3, 0.67 mM $NH_4H_2PO_4$, 2 mM $MgSO_4 \cdot 7H_2O$, 0.05 mM H_3BO_3, 0.009 mM $MnSO_4 \cdot 4H_2O$, 0.7 mM $ZnSO_4 \cdot 7H_2O$, 0.32 mM $CuSO_4 \cdot 5H_2O$, 0.1 mM

$(NH_4)^2MoO_4$, 0.05 mM $FeSO_4 \cdot 7H_2O$, and 0.04 mM Na_2-EDTA. The pH was adjusted to 5.8 $\pm$ 0.1 as required. The nutrient solution was replaced once every 3 days. At the vegetative growing stage (30 days), K^+ deficiency treatment was applied by reducing the concentration of KNO_3 from 4 mM (normal K^+) to 0.5 mM (K^+ deficiency) in the nutrient solution. A concentration of 4 mM KNO_3 was used as a control. After 7 days of K^+ deficiency stress, different parts of the plant were sampled and dried to assess plant root configuration, dry weight, and K^+ content.

Measurement of K^+ concentrations

First, 0.05 g dry weight tomato roots was added to a 10-mL centrifuge tube containing 2 mL of 0.5 M

hydrochloric acid. Samples were incubated for 3 days, after which, 5 mL deionised water was added to each centrifuge tube, and the mixture was filtered. The filtered stock solution was diluted 10 times, and the K^+concentration was measured with a flame photometer. Each sample was evaluated with three biological replicates.

35S:miR-168a and 35S:rSlAGO1 vector construction and tomato transformation

Pre-SlmiR-168a was prepared using gene-specific primers. The sequence-confirmed polymerase chain reaction (PCR) fragment was cloned into pCAMBIA3301/Luc, which harboured two 35S Cauliflower mosaic virus promoters, the marker gene for kanamycin resistance, phosphinothricin, and luciferase. The bacterial colonies were screened for positive recombinant plasmids by colony PCR, restriction enzyme digestion, and sequence analysis. Binary vectors containing the expected insert were subsequently transferred into *Agrobacterium tumefaciens* GV3101 cells by electroporation. The competent cells harbouring the vector were transformed into JZ18 tomatoes using a tomato genetic transformation system. The obtained T1 transformants and their corresponding T2 families were assessed for the expression of the target gene by quantitative real-time PCR (qRT-PCR) and evaluation of the presence of the kanamycin marker gene. All primers used in this study are listed in Supplementary Table S1. To generate *rSlAGO1* (the*SlmiR-168a* -resistant construct), mutations in the*SlmiR-168a* target site of *SlAGO1* were inserted using two-step PCR mutagenesis. The *35S:SlAGO1* transformants were obtained using the same method as described above.

Small RNA sequencing and analysis of differentially expressed miRNAs

35S:SlmiR-168a , *35S:rSlAGO1* , and JZ18 were used as small RNAs. In total, nine samples (*35S:SlmiR-168a* , *35S:rSlAGO1* , and JZ18, each with three replicates) were harvested. Approximately 2.5 μg total RNA was used to prepare a small RNA library using a TruSeq Small RNA Sample Prep Kit (Illumina, San Diego, CA, USA) according to the manufacturer's instructions. The libraries were then sequenced using an Illumina Hiseq2500 50SE (single end) at LC-BIO (Hangzhou, China) following the vendor's recommended protocol. Briefly, raw reads were subjected to the Illumina pipeline filter (Solexa 0.3), and the dataset was then further processed with an in-house program, ACGT101-miR (LC Sciences, Houston, TX, USA), to remove adapter dimers, junk, low complexity, common RNA families (rRNA, tRNA, snRNA, and snoRNA), and repeats. Subsequently, unique sequences 18–26 nt in length were mapped to specific species precursors in miRBase 21.0 by Bowtie search to identify known miRNAs and novel 3p- and 5p-derived miRNAs. Length variation at both the 3' and 5' ends and one mismatch inside of the sequence were allowed in the alignment. Mapping methods for the identification of conserved and novel miRNAs are listed in Table S2.

Prediction of target genes of miRNAs

To predict the genes targeted by differentially expressed miRNAs, two computational target prediction algorithms (TargetScan 50 and miRanda 3.3a) were used to identify miRNA binding sites. Finally, the data predicted by both algorithms were combined, and the overlaps were calculated.

Transcriptome sequencing, annotation, and analysis

Tomato leaflet samples were collected from JZ8, *35S:rSlAGO1* , and*35S:SlmiR-168a* at the same stage and position on the plants, and an Illumina Miseq library was constructed (Illumina), according to the manufacturer's instructions. Magnetic beads with poly T oligos attached were used to purify the mRNA from the total RNA. Fragmentation buffer was added to cleave the mRNA into short fragments, and the fragments were used to synthesise first-strand cDNA using random hexamer primers. The cDNA was transformed into double-stranded cDNA with RHase H and DNA polymerase I, and a paired end library was constructed from the synthesised cDNA with a Genomic Sample Prep Kit (Illumina). Fragments of desirable lengths were purified with a QIAquick PCR Extraction Kit (Qiagen, Valencia, CA, USA), end repaired, and linked with sequencing adapters (Margulies et al. 2005). AMPureXP beads were used to remove the unsuitable fragments, and the sequencing library was the constructed by PCR amplification. Libraries were checked with PicoGreen staining and fluorospectrophotometry, quantified with an Agilent 2100 instrument, and mixed in equal volumes to a normalised concentration of 10 nM. The sequencing library was then sequenced using the

Illumina Miseq platform (LC-BIO Technology Co., Ltd.).

Integrated analysis of mRNA-seq and miRNA-seq data

In order to define all possible miRNA/mRNA interactions, including positive and negative relationships between miRNA and mRNA expression, we used ACGT101-CORR 1.1 to construct the miRNA/mRNA regulatory network. Briefly, we normalised all the sample-matched miRNA and mRNA sequencing data. Integration of miRNA-seq with mRNA-seq data was then achieved by integrating profiles of differentially expressed miRNAs and mRNAs with the addition of differentially expressed miRNA-targeting information.

qRT-PCR analysis

Total RNA from the samples was extracted using TRIzol (Takara, Dalian, China) followed by an RNasefree treatment (Takara). The RNA (4 μg) was pretreated with RQ1 Dnase I (Promega, Madison, WI, USA) to remove contaminating genomic DNA. Total RNA concentrations were measured using a NanoDrop instrument (Thermo Fisher Scientific, Waltham, MA, USA), and RNA quality was checked using nondenaturing agarose gel electrophoresis. Total DNA-free RNA (2 μg) was used for cDNA synthesis in a total volume of 40 μL, and the resulting cDNA was used as the template for RT-PCR. PCR for the target mRNAs was carried out in 20-μL reactions containing 2 μL cDNA synthesis reaction mixture, 400 nM each primer, and 10.5 μL SYBR Green PCR Master Mix (TianGen Biotech, Beijing, China) on an ABI 7500 sequence detection system (Applied Biosystems, Foster City, CA, USA). The main feature of mature miRNA expression detection is the RT primer, which has a stem loop structure and a consensus sequence that effectively binds to the 3'end of the miRNA. PCR for the mature miRNAs was carried out in 25-μL reactions containing 2.5 μL cDNA synthesis reaction mixture, 400 nM each primer, and 12.5 μL SYBR Green PCR Master Mix. In addition, each measurement was repeated using three technical replicates, in which the RNA samples were mixed with three biological replicates. The gene primers are listed in Supplementary Table S1.

CTK and abscisic acid (ABA) quantification

CTK and ABA were quantified using the following enzyme-linked immunosorbent assay protocol (Yang et al. 2001). Briefly, samples were homogenised in liquid nitrogen and extracted in cold 80% (v/v) methanol with butylated hydroxytoluene (1 mM) overnight at 4°C. The extracts were collected after centrifugation at 10000 × *g* (4°C) for 20 min, passed through a C18 Sep-Pak cartridge (Waters, Milford, MA, USA), and dried in N_2. The residues were dissolved in phosphate-buffered saline (0.01 M, pH 7.4) to determine the CTK and ABA levels. Microtitration plates were coated with synthetic CTK or ABA-ovalbumin conjugates in $NaHCO_3$ buffer (50 mM, pH 9.6) and left overnight at 37°C. Ovalbumin solution (10 mg/mL) was added to each well to block nonspecific binding. After incubation for 30 min at 37°C, standard CTK and ABA, samples, and antibodies were added and incubated for an additional 45 min at 37°C. Antibodies against CTK and ABA were obtained as described by Weiler et al. (1981). Then, horseradish peroxidase-labelled goat anti-rabbit immunoglobulin was added to each well, and samples were incubated for 1 h at 37°C. Finally, the buffered enzyme substrate (orthophenylenediamine) was added, the enzyme reaction was carried out in the dark at 37°C for 15 min, and the reaction was then terminated using 3 M H_2SO_4. The absorbance was recorded at 490 nm. Calculations of the enzyme immunoassay data were performed as described by Weiler et al. (1981).

Statistical analysis

At least three biological replicates were performed; the data are presented as the mean ± SD. Significance tests were carried out in SPSS software (version 17.0) based on Student's t-tests at $P < 0.01$ or $P < 0.05$ or One-Way ANOVA by Duncan's method at $P < 0.05$.

Results

Differential expression of SlmiR-168a and SlAGO1 in JZ18 and JZ34

JZ34 tomatoes (low-K^+ tolerant) show better root development and K^+ absorption ability than JZ18 tomatoes (low-K^+ sensitive) under K^+deficiency (Zhao et al. 2018). According to our previous miRNA-seq research,

SlmiR-168a is differentially expressed between JZ18 and JZ34 tomatoes under K^+ deficiency stress. Therefore, in this study, we first performed RT-PCR to show that the expression levels of *SlmiR-168a* were increased with time in JZ18 tomatoes under normal conditions. However, we found that *SlmiR-168a* levels were decreased under K^+ deficiency with time (Fig. 1a), suggesting that in low K^+-sensitive JZ18,*SlmiR-168a* expression affected the tolerance of tomatoes to K^+ deficiency. Corresponding expression patterns were observed for the *SlmiR-168a* target gene *SlAGO1* after treatment for 3 and 5 days (Fig. 1b). However, in JZ34 tomatoes, the expression levels of *SlmiR-168a* were significantly increased by K^+ deficiency, particularly after treatment for 3, 5, and 7 days (Fig. 1c). The target AGO1 expression levels were obviously decreased under K^+ deficiency compared with that under normal conditions in JZ34 tomatoes (Fig. 1d). As a target of*miR-168a* , *SlAGO1* showed a complementary expression pattern, and the expression of *SlmiR-168a* actually responded to the low K^+ stress. The differential expression patterns of *SlmiR-168a* between JZ18 and JZ34 tomatoes may be a cause of the variations in tolerance of the two tomato genotypes under low K^+ stress.

Analysis of SlmiR-168a and SlAGO1 expression in different tissues of tomato plants

The expression of *SlmiR-168a* and *SlAGO1* in different tissues of tomato plants was evaluated by RT-PCR (Fig. 2).*SlmiR-168a* and *SlAGO1* were detected in all tissues. The expression levels of *SlmiR-168a* were the highest in the leaves and flowers, followed by the roots and stems. In the stems, leaves, and flowers, *SlAGO1* showed the opposite expression pattern compared with *miR-168a* .

Regulation of SlAGO1 by SlmiR-168a increased plant tolerance to K^+ deficiency stress

To elucidate whether the regulation of *SlAGO1* by*SlmiR-168a* was responsible for differences in low K^+ tolerance, transformants of *35S:SlmiR-168a*and *35S:rSlAGO1* were obtained. *SlmiR-168a* -resistant constructs (*rSlAGO1*) were generated using a point mutation (Fig. 3a). This mutation did not change the native protein sequence of*SlAGO1* . The *rSlAGO1* and *pre-SlmiR-168a* fragments were amplified by PCR for overexpression vector construction (Fig. 3b and c). *35S:SlmiR-168a* and *35S:rSlAGO1* transformants were obtained for subsequent experiments. The root morphology of WT,*35S:SlmiR-168a* , and *35S:rSlAGO1* all showed a larger root system after 7 days of development at the normal K^+concentration (4 mM) (Fig. S5). However, in the presence of a low K^+ concentration (0.5 mM), the roots of*35S:SlmiR-168a* plants appeared stronger than WT and*35S:rSlAGO1* plants after 7 days of treatment. Microexamination revealed that the number of root hairs was obviously increased in*35S:SlmiR-168a* plants following low K^+treatment at 7 days compared with that in WT and *35S:rSlAGO1*plants (Fig. 4a). Leaf development was also observed under K^+ deficiency stress (Fig. 4b). The leaf margins of JZ18 control plants turned yellow under low K^+conditions, and those of *35S:rSlAGO1* plants showed increased yellowing; in contrast, *35S:SlmiR-168a* plants did not exhibit yellowing of the leaves. Analysis of the root-shoot ratio (Fig. 4c) showed that under low K^+ conditions, root-shoot ratios of *35S:SlmiR-168a* plants did not differ significantly compared with that in WT plants. However, *35S:rSlAGO1* plants exhibited a decreased root-shoot ratio compared with WT and *35S:SlmiR-168a*plants. Additionally, the chlorophyll content was highly increased in*35S:SlmiR-168a* plants but decreased in WT and *35S:rSlAGO1*plants under K^+ deficiency stress (Fig. 4d). Chlorophyll contents in *35S:rSlAGO1* plants were also lower than that in WT plants under both normal K^+ and low K^+ conditions. Analysis of K^+contents in roots (Fig. 4e) showed that under normal K^+ concentration conditions, *35S:SlmiR-168a*plants showed increased K^+ contents with development time, particularly after 7 days of treatment. *35S:SlmiR-168a*plants also showed higher K^+ contents than WT plants after 7 days, whereas *35S:rSlAGO1* plants exhibited lower K^+ contents than WT plants. Under low K^+ concentration conditions, *35S:SlmiR-168a*plants exhibited improved root and leaf growth, whereas*35S:rSlAGO1* showed weaker root and leaf growth. Moreover,*35S:SlmiR-168a* plants exhibited higher K^+contents in roots under K^+ deficiency stress.

Analysis of miRNA sequencing data in 35S:SlmiR-168a and 35S:rSlAGO1 plants

To identify miRNAs regulated by *SlmiR-168a* -mediated *SlAGO1*in response to K^+ deficiency stress, nine small RNA libraries were constructed from WT, *35S:SlmiR-168a* , and*35S:rSlAGO1* samples. In total, 12,836,013, 14,373,027, 13,912,496, 14,850,199, 17,821,390, 12,006,556, 17,470,288, 12,383,616, and 25,030,158

raw reads were generated by high-throughput sequencing for the three genotypes and three replicates (Table S2). After data processing, including filtration of small RNAs except miRNAs, 7,163,035, 11,223,930, 9,849,836, 8,542,869, 10,694,993, 7,571,073, 10,723,320, 9,305,655, and 16,653,370 total valid reads, corresponding to 2,575,545, 4,694,297, 4,410,072, 3,159,839, 3,691,188, 2,895,817, 3,862,724, 4,199,533, and 5,3931,63 unique reads were acquired in the libraries of WT, *35S:SlmiR-168a* , and*35S:rSlAGO1* plants (with three replicates each), respectively. The majority of valid reads were 20–24 nt in length, with 24-nt reads being the most common among all three genotypes (Fig. 5a). In total, we identified 1168 conserved miRNAs belonging to miRNA families and 1060 predicted novel miRNAs in the nine small RNA libraries (Table S3). Details regarding family member numbers of conserved miRNA are summarised in Table S4. Overall, 68 conserved miRNA families contained more than one member.

Identification of miRNAs expressed in the two transgenic tomato plants

When comparing *35S:SlmiR-168a* plants with WT plants, 122 miRNAs were significantly upregulated (fold change > 2; $P< 0.1$), whereas 110 miRNAs were significantly downregulated (fold change > 2; $P < 0.1$; Fig. 5b; Table S5). When comparing *35S:rSlAGO1* plants with WT plants, 102 miRNAs were significantly upregulated (fold change > 2; $P< 0.1$), whereas 58 miRNAs were significantly downregulated (fold change > 2; $P < 0.1$; Fig. 5b; Table S6). There were 334 miRNAs that were upregulated in the comparison of*35S:rSlAGO1* and WT plants but downregulated in the comparison of*35S:SlmiR-168a* and WT plants (Table S7). There were 276 miRNAs that were downregulated in the comparison of *35S:rSlAGO1* and WT plants but upregulated in the comparison of *35S:SlmiR-168a* and WT plants (Table S7).

Function analysis of miRNA predicted targets

Putative targets for 107 differentially expressed miRNAs were identified (Table S8), and the identified target genes are listed in Table S9. Gene ontology (GO) enrichment analysis for the predicted targets of the 107 miRNAs identified 20 terms, including nucleus, plasma membrane, and ATP binding, that changed significantly ($P < 0.00015$) between the two transgenic tomato plants compared with those in the WT plants (Fig. 6a). Pathway enrichment analysis for the predicted targets of the 107 miRNAs identified 20 pathways, including ABC transporters, glycerophospholipid metabolism, circadian rhythem-plant, and RNA degradation, that changed significantly ($P < 0.05$) between the two transgenic tomato plants compared with those in the WT plants (Fig. 6b).

Correlation of differentially expression miRNAs and mRNAs from 35S:SlmiR-168a and 35S:rSlAGO1 plants compared with WT plants

There is a regulatory relationship between miRNAs and mRNAs, and this relationship can be established through target gene prediction. In this study, we found 113 miRNA/mRNA pairs in the comparison of*35S:SlmiR-168a* and WT plants, with both positive and negative correlations (Table S10), and 93 miRNA/mRNA pairs in the comparison of*35S:rSlAGO1* and WT plants, with both positive and negative correlations (Table S11). Owing to various regulatory factors, the expression of mRNAs by miRNAs did not have a completely inverse relationship, and both positive and negative correlations were detected. For most cases involving target cleavage, the simple expectation is that when miRNAs are induced, the expression levels of their target mRNAs are reduced and vice versa. There were 74 negative miRNA/mRNA interactions in the comparison of *35S:SlmiR-168a* with WT (Table S10) and 49 negative miRNA/mRNA interactions in the comparison of *35S:rSlAGO1*with WT (Table S11). Although AGO1 is known to be important for the stabilisation of miRNAs, its role in miRNA production has not been established (Vaucheret et al. 2004). However, our findings identified 10 upregulated miRNA and downregulated mRNA interaction pairs in the comparison of *35S:rSlAGO1* with WT and two downregulated miRNA and upregulated mRNA interaction pairs in the comparison of*35S:SlmiR-168a* with WT (Table 1). Thus, these miRNAs were thought to be stabilised by AGO1 protein. GO analysis of the 12 negative miRNA/mRNA pairs identified 28 functional processes that involved the CTK-activated signalling pathway, responses to salt stress, and responses to ABA (Figs. S1 and S3). Additionally, pathway enrichment analysis of the 12 negative miRNA/mRNA pairs identified four pathways, including plant/pathogen interactions, plant hormone signal transduction, base excision repair,

and histidine metabolism (Fig. S2).

RT-PCR validation of differentially expressed miRNAs and mRNAs

The expression profiles of 10 differentially expressed mature miRNAs (*stu-miR530_L-2R+2* , *stu-miR-8039_-R+3_1ss4CT* ,*stu-miR-384-5p_R+1* , *ppe-miR-858_1ss4GA* ,*ath-miR-171a-3p_L-3R+1* , *PC-3p-276756_24* ,*PC-5p-289257_23* , *PC-5p-66618_119* ,*stu-miR-8006-p3_1ss8GA_1* , and *stu-miR-8007b-p3_1ss22CT*) and 12 differentially expressed target genes (*Solyc04g008110.3.1* ,*Solyc07g063510.3.1* , *Solyc03g113890.1.1* ,*Solyc06g076850.3.1* , *Solyc05g006420.3.1* ,*Solyc08g069180.3.1* , *Solyc12g056040.1.1* ,*Solyc05g006420.3.1* , *Solyc04g082420.3.1* ,*Solyc08g066260.3.1* , *Solyc09g097780.2.1* , and*Solyc09g064820.1.1*) were further validated using qRT-PCR (Table 1). The results of qRT-PCR revealed that most of these miRNAs/mRNAs shared similar expression patterns as those observed in the miRNA-Seq/mRNA-Seq data (RPKM/reads-based expression values; Tables S10 and S11). Although there were some quantitative differences between the two analytical platforms, the similarities between the sequencing data and qRT-PCR suggested that the data were reliable.

Identification of miRNAs responsive to K^+ deficiency stress

From the 10 differentially expressed mature miRNAs, seven known miRNAs were chosen to detect their expression under K^+deficiency stress by RT-PCR (Fig. 7). In the low K^+sensitive genotype tomato 'JZ18', the expression levels of*stu-miR08006* and *stu-miR-8007b* were decreased after low K^+ treatment for 12 h. *Ppe-miR858* ,*stu-miR-384* , *ath-miR-171a* , *stu-miR-8039* , and*stu-miR-530* expression levels were all upregulated after low K^+ treatment for 3 days in JZ18 tomatoes. In the low K^+ tolerant genotype tomato 'JZ34',*stu-miR-8006* expression was significantly increased after low K^+ treatment for 3 and 5 days, whereas*stu-miR-8007b* expression was increased after low K^+ treatment for 12 h and 3 days. In contrast,*ppe-miR-858* , *stu-miR-384* , *ath-miR-171a* ,*stu-miR-8039* , and *stu-miR-530* expression levels tended to decrease following low K^+ treatment in JZ34. Taken together, these findings suggested that *stu-miR-8006* and*stu-miR-8007* positively responded to K^+deficiency stress in low K^+ tolerant tomatoes, whereas*ppe-miR-858* , *stu-miR-384* , *ath-miR-171a* ,*stu-miR-8039* , and *stu-miR-530* negatively responded to K^+ deficiency stress in low K^+tolerant tomatoes.

Differences in CTK/ABA production between genotypes under K^+ deficiency stress

Low K^+ sensitive JZ18 tomatoes and low K^+ tolerant JZ34 tomatoes (Zhao et al. 2018) were measured to show differences in CTK and ABA contents under K^+ deficiency stress (Fig. 8). Under K^+-deficiency stress, the CTK contents of JZ34 were significantly higher than those of JZ18 as treatment time increased (Fig. 8a). However, under normal conditions, the CTK contents were lower in JZ34 plants than in JZ18 plants. Under K^+deficiency stress, the ABA contents of JZ34 were also significantly higher than those in JZ18 as treatment time increased (Fig. 8b). Thus, CTK/ABA contents both increased in low K^+ tolerant JZ34 plants under K^+ deficiency stress.

Discussion

Regulation of SlAGO1 by SlmiR-168a mediated root development in response to K^+ deficiency stress

K^+ deficiency in soil is of great agricultural importance (Laegreid et al. 1999). One important aspect of plant adaptation to K^+ deficiency stress is cellular and tissue homeostasis of K^+, which involves transport of K^+ across various membranes in several tissues (Amtmann et al. 2005). The two tomato genotypes (low K^+ tolerant JZ34 and low K^+sensitive JZ18) exhibit marked differences in sensitivity to K^+ deficiency and root morphology (Zhao et al. 2018). Moreover, JZ34 has more root hairs under K^+ deficiency treatment than JZ18 and exhibits stronger nutritional uptake capability of K^+ than JZ18 (Zhao et al. 2018). Thus, JZ34 maintains higher K^+ contents under K^+deficiency stress than JZ18. In our current study, the expression of*SlmiR-168a* was increased in response to low K^+, whereas the expression of its target *SlAGO1* was decreased following low K^+ treatment (Fig. 1). Both*SlmiR-168a* and *SlAGO1* were expressed at higher levels in roots than in other tissues (Fig. 2). Additionally,*35S:SlmiR-168a* had more root hairs than *35S:rSlAGO1* and JZ18 (Fig

.4a). Notably, the potassium deficiency signal is first perceived by root cells, particularly root epidermal cells and root hair cells (Song et al. 2017).

Integrated analysis of mRNA-Seq and miRNA-Seq results in*35S:rSlAGO1* showed that a member of the *miR-171* family was significantly induced and that its target *Solyc08g069180.3.1* was downregulated (Table 1). Further analysis showed that this target gene was involved in root epidermal cell differentiation and stress responses. Previous studies have shown that *miR-171* expression is higher in the vascular bundle and cuticle layer of roots in*Arabidopsis* (Mahale et al. 2014) and that this miRNA is upregulated in response to Cd stress, drought, and salt stress (Liu et al. 2008; Zhou et al. 2008). *miR-171* has also been shown to be differentially expressed in maize roots in response to salt stress (Ding et al. 2009). Therefore, we concluded that regulation of*Solyc08g069180.3.1* by *miR-171a* may explain differences in root development between *35S:SlmiR-168a* and *35S:rSlAGO1* under K^+ deficiency stress (Fig. 9).

SlmiR-168a regulated SlAGO1-mediated CTK/ABA signalling in response to K^+ deficiency stress

In addition to root architecture, phytohormones also are involved in signal transduction of plant responses to K^+deficiency stress. Low K^+ stress results in decreased CTK levels, which may stimulate ROS accumulation, root hair growth, and*AtHAK5* expression (Nam et al. 2012). The KAT1 potassium channel is a target for ABA signal transduction through SRK1/OST1/SnRK2.6 (Sato et al. 2009).

Additionally, expression of the K^+ release channel gene *GORK* is induced by ABA in the presence of extracellular Ca^{2+} (Becker et al. 2003). In this study, we found that the low K^+ tolerant tomato JZ34 had higher CTK/ABA contents under K^+ deficiency stress than the low K^+ sensitive tomato JZ18.

Integrated analysis of mRNA-Seq and miRNA-Seq results for the comparison of *35S:rSlAGO1* versus JZ18 showed that *miR-384* , *miR-530* , and *miR-858* were upregulated and that their downregulated targets were enriched in the CTK signalling pathway and CTK responses. Moreover, we found that targets of *miR-384* , *miR-530* , and*miR-858* were also involved in plant hormone signal transduction. Additionally, target genes of the novel miRNA*PC-3p-276756_24* were found to be involved in CTK responses. Interestingly, in *35S:SlmiR-168a* , only *miR-8006* and *miR-8007b* were downregulated, and their upregulated targets were enriched in response to salt stress and ABA. Accordingly, our results showed that *SlAGO1* induced the expression of various miRNAs, including *miR-384* , *miR-530* ,*miR-858* , *miR-8007* , and *PC-3p-276756_24* , through regulation of *SlmiR-168a* . These miRNA/mRNA pairs may influence tolerance to K^+ deficiency stress in plants via the CTK/ABA signalling pathway (Fig. 9). CTK- and ABA-related genes that were downregulated in *35S:rSlAGO1* and upregulated in*35S:SlmiR-168a* are listed in Table S12.

K^+ transport via ABA signalling requires extracellular Ca^{2+} (Becker et al. 2003), and P68 protein combines with AGO1 to interact with CaM and enhance accumulation of K^+ in rice (Banu et al. 2015). Thus, P68 expression was investigated in *35S:SlmiR-168a* and *35S:rSlAGO1* (Fig. S4). P68 expression levels were decreased in *35S:rSlAGO1* but increased in *35S:SlmiR-168a* compared with those in JZ18. Based on these findings, the pathway through which *SlAGO1* was regulated by*SlmiR-168a* in response to K^+ deficiency stress via ABA signalling may require Ca^{2+}.

Function of AGO1 in the miRNA regulatory pathway

miRNAs are loaded onto *AGO1* , which acts as an RNA slicer in plants (Baumberger and Baulcombe, 2005). *miR-168* directs the cleavage of *AGO1* mRNA, indicating that *miR-168* regulates the activity of its own miRNA pathway (Vaucheret et al. 2004).*AGO1* -null alleles reduce the expression levels of some miRNAs, such as *miR-171* , and increase the levels of the corresponding target mRNAs (Vaucheret et al. 2004). In *35S:rSlAGO1* , eight miRNAs were upregulated, and their targets were downregulated. Moreover, in *35S:SlmiR-168a* , *miR-8006* and *miR-8007* were downregulated, and their targets were upregulated. Thus, these miRNAs may be associated with AGO1 protein, and impairment of AGO1 expression could decrease the expression levels of these miRNAs, resulting in upregulation of their targets to affect the plant response to the environment. Additionally, in *35S:SlmiR-168a* , 71 miRNAs were upregulated, and their targets were downregulated. These miRNAs included many widely known molecules, such as *miR-167* , *miR-156* ,*miR-*

396 , *miR166* , *miR-319b* , and *miR-172* . These miRNAs may be involved in various hormone signalling pathways, including auxin, ethylene, and gibberellin signalling. In*AGO1*- null plants, *miR-156 /-157* and *miR-167*were found to accumulate to levels similar to or higher than those in WT plants (Vaucheret et al. 2004). Furthermore, Lynn et al. (1999) reported that PINHEAD/ZWILLE is 75% similar to and has overlapping functions with AGO1. miRNAs regulatory network is not only relying on AGO but also other proteins. AGO proteins can bind to single-stranded RNAs that are at least 5 nt in length and to double-stranded RNA, enabling AGO protein to directly associate with miRNAs before and after they recognise their mRNA targets (Yan et al. 2003). Importantly, miRNAs are regulated by AGO in time and space fine-tuned and complex regulatory networks. Thus,*miR-168* may function with AGO1 to control the mRNA levels of miRNA targets through a complex pathway.

Regulatory network of miRNA/mRNA by miR-168a-mediated SlAGO1 and K^+ deficiency stress tolerance

Based on analysis of miRNAs and mRNAs responding to K^+deficiency stress, we developed a model of *miR-168* -mediated AGO1 function in low K^+ tolerance (Fig. 9). *SlAGO1*is regulated by *SlmiR-168a* in response to K^+deficiency stress, and *SlAGO1* protein then induces the expression of *miR-530* , *miR-384* , *miR-858* , and*PC-3p-276756_24* , resulting in inhibition of the targets of these miRNAs, which participate in CTK signalling. *SlAGO1* also induces*miR-171* expression and downregulates its targets, which are involved in root epidermal cell differentiation. Moreover,*SlmiR-168a* -mediated *SlAGO1* regulates the expression of*miR-8007* , which is involved in the ABA signalling pathway; Ca^{2+} may have functions in this pathway as well.

Overall, our findings demonstrated that *SlmiR-168a* mediated*SlAGO1* expression in response to K^+ deficiency stress, resulting in modulation of root growth and CTK/ABA signalling. Other hormonal or regulatory pathways may be involved as well, necessitating further studies. However, our results clearly revealed the new roles of *SlmiR-168a* -mediated *SlAGO1* in the response to low K^+ stress and highlighted the importance of*SlAGO1* in maintaining the homeostasis of miRNA accumulation. Although further studies are needed to elucidate the detailed mechanisms of the miRNA targets mediated by low K^+ stress responses, our study provided important insights into plant stress regulatory pathways and improved our understanding of*miR-168* -mediated AGO1 function in response to low K^+.

Acknowledgements

This work was supported by grants from the National Key Research and Development Program of China (2019YFD1000300), the National Natural Science Foundation of China (31801847) and the Doctor Started Fund of Liaoning Province(20180540059). The authors have no conflict of interest to declare. We would like to thank Editage (www.editage.cn) for English language editing.

Conflicts of Interest: The authors declare no conflict of interest.

Figure Legends

Figure 1. *SlmiR-168a* and *SlAGO1* expression profiles in JZ18 and JZ34 plants under normal K^+conditions and K^+ deficiency conditions. Samples were collected at 0, 1, 3, 5, and 7 days after treatment. a. JZ18 seedlings under normal K^+ conditions; b. JZ18 seedlings under K^+ deficiency conditions; c. JZ34 seedlings under normal K^+ conditions; d. JZ34 seedlings under K^+ deficiency conditions. CK: normal K^+ (4 mM); LK: K^+ deficiency (0.5 mM). The experiments were repeated three times. $^*P < 0.05$ compared with the control.

Figure 2. *SlmiR-168a* and *SlAGO1* expression profiles in different tomato tissues. The experiments were repeated three times. $^*P < 0.05$ compared with the control.

Figure 3. Mutant *SlAGO1* transgenic transcripts were resistant to *SlmiR-168a* -mediated cleavage in tomatoes. a. Representation of the constructs used for transgenic expression of the*SlmiR-168a* -resistant mutant (*rSlAGO1*) in tomatoes. Mutations were introduced at four locations, and these base changes did not affect the native protein sequence. b. Amplification of the*rSlAGO1* cDNA band located at 3100 bp. c. Amplification of the*pre-SlmiR-168a* band at 159 bp.

Figure 4. Comparison of morphological changes in WT,*35S:SlmiR-168a* , and *35S:rSlAGO1* plants under normal K^+ conditions and K^+ deficiency stress after 7 days. a. Changes in the root hair region in WT,*35S:SlmiR-168a* , and *35S:rSlAGO1* plants under CK and LK conditions after 7 days (100×magnification). b. Differences in leaflet states in WT, *35S:SlmiR-168a* , and *35S:rSlAGO1* plants under CK and LK conditions after 7 days. c. Root-shoot ratios in WT,*35S:SlmiR-168a* , and *35S:rSlAGO1* plants under CK and LK conditions after 7 days. d. Chlorophyll contents of WT,*35S:SlmiR-168a* , and *35S:rSlAGO1* plants under CK and LK conditions after 7 days. e. K^+ contents in WT,*35S:SlmiR-168a* , and *35S:rSlAGO1* plants under CK and LK conditions after 3 and 7 days. CK: normal K^+ (4 mM); LK: K^+ deficiency (0.5 mM).

Figure 5. The identified miRNAs from WT, *35S:SlmiR-168a* , and *35S:rSlAGO1* plants. a. Length distribution of total identified miRNAs. b. Number of miRNAs in *35S:rSlAGO1* plants compared with WT and *35S:SlmiR-168a* plants compared with WT.$P < 0.05$, 0.01, or 0.001.

Figure 6. a. GO analysis of predicted targets of 107 differentially expressed miRNAs (20 terms). b. KEGG pathway enrichment analyses of predicted targets of 107 differentially expressed miRNAs (20 pathways).

Figure 7. Quantitative real-time PCR validation of seven differentially expressed miRNAs in low K^+ sensitive JZ18 tomatoes and low K^+ tolerant JZ34 tomatoes under normal conditions and K^+ deficiency stress. K^+: normal K^+ (4 mM); K^-: K^+ deficiency (0.5 mM). The experiments were repeated three times.

Figure 8. Comparison of CTK and ABA contents in low K^+ sensitive and low K^+ tolerant tomatoes under K^+ deficiency stress conditions after 24 h, 3 days, and 7 days. CK: normal K^+ (4 mM); LK: K^+ deficiency (0.5 mM). The experiments were repeated three times. $^*P < 0.05$.

Figure 9. Hypothetical model of the molecular mechanisms through which *SlmiR-168a* -mediated *SlAGO1* regulates the K^+ deficiency stress response. *SlAGO1* regulated by *SlmiR-168a* may be involved in various processes, including root growth, the CTK signalling pathway, and the ABA signalling pathway, by influencing the regulatory pathways of other miRNAs (e.g.,*ath-miR-171a* , *stu-miR-530* , *stu-miR-0384* ,*ppe-miR-858* , *stu-miR-8007b* , and *PC-3p-276756_24*).

Supporting Information

Additional Supporting Information may be found in the online version of this article at the publisher's web-site:

Table S1. Primers used in this study.

Table S2. The profiles of small RNA deep sequencing for 35S:SlmiR168a, 35S:rSlAGO1 and WT.

Table S3. List of all expressed miRNA in *35S:SlmiR-168a* ,*35S:rSlAGO1* and WT.

Table S4. The expressed conserved miRNAs were classified into different miRNAs families.

Table S5. List of the differentially expressed miRNAs in*35S:SlmiR-168a* plants compared with WT.

Table S6. List of the differentially expressed miRNAs in*35S:rSlAGO1* plants compared with WT.

Table S7. 334 miRNAs that were upregulated in the comparison of*35S:rSlAGO1* and WT plants but downregulated in the comparison of*35S:SlmiR-168a* and WT plants ; 276 miRNAs that were downregulated in the comparison of *35S:rSlAGO1* and WT plants but upregulated in the comparison of *35S:SlmiR-168a* and WT plants.

Table S8. List of the miRNAs whose target geFnes are predicted.

Table S9. Target predict annotation for the differentially expressed miRNAs.

Table S10. miRNA/mRNA pairs in the comparison of *35S:SlmiR-168a* and WT plants, with upregulated/upregulated, downregulated/downregulated, upregulated/downregulated, downregulated/upregulated by integrated analysis of miRNA-Seq and mRNA-Seq.

Table S11. miRNA/mRNA pairs in the comparison of*35S:rSlAGO1* and WT plants, with upregulated/upregulated, downregulated/downregulated, upregulated/downregulated, downregulated/upregulated by integrated analysis of miRNA-Seq and mRNA-Seq.

Table S12. List of the CTK- and ABA-related genes that were downregulated in *35S:rSlAGO1* and upregulated in*35S:SlmiR-168a* .

Figure S1. GO analyses of the 10 negative miRNA/mRNA pairs identified in the comparison of*35S:rSlAGO1* and WT plants by integrated analysis of miRNA-Seq and mRNA-Seq.

Figure S2. KEGG pathway enrichment analyses of the 10 negative miRNA/mRNA pairs identified in the comparison of *35S:rSlAGO1* and WT plants by integrated analysis of miRNA-Seq and mRNA-Seq.

Figure S3. GO analyses of the 2 negative miRNA/mRNA pairs identified in the comparison of *35S:SlmiR-168a* and WT plants by integrated analysis of miRNA-Seq and mRNA-Seq.

Figure S4. Quantitative real-time PCR validation of P68 in*35S:SlmiR-168a* , *35S:rSlAGO* and WT. The experiments were repeated three times.

Figure S5. Comparison of morphological changes of root growth in WT, *35S:SlmiR-168a* , and *35S:rSlAGO1* plants under normal K^+ conditions and K^+ deficiency stress after 7 days.

References

Amtmann, A., Hammond, J.P., Armengaud, P. & White, P.J. (2005). Nutrient sensing and signalling in plants: potassium and phosphorus.*Advances in Botanical Research* , 43, 209-257.

Banu, M.S.A., Huda, K.M.K., Sahoo, R.K., Garg, B., Tula, S., Islam, S.M.S., Tuteja, R. & Tuteja, N. (2015). Pea p68 imparts salinity stress tolerance in Rice by scavenging of ROS-mediated H_2O_2 and interacts with Argonaute.*Plant Molecular Biology Reporter* , 33, 221-238.

Baumberger, N. & Baulcombe, D.C. (2005). Arabidopsis ARGONAUTE1 is an RNA slicer that selectively recruits microRNAs and short interfering RNAs. *Proc. Natl. Acad. Sci. USA* , 102, 11928-11933.

Becker, D., Hoth, S., Ache, P., Wenkel, S., Roelfsema, M.R.G., Meyerhoff, O., Hartung, W. & Hedrich, R. (2003). Regulation of the ABA-sensitive Arabidopsis potassium channel gene GORK in response to water stress. *FEBS Letters* , 554, 119-126.

Behera, S., Long, Y., Schmitz-Thom, I., Wang, X.P., Zhang, C., Li, H., Steinhorst, L., Manishankar, P., Ren, X.L., Offenborn, J.N., Wu, W.H., Kudla, J. & Wang, Y. (2017). Two spatially and temporally distinct Ca^{2+} signals convey *Arabidopsis thaliana*responses to K^+ deficiency. *New Phytol* , 213, 739-750.

Besford, R.T. & Maw, G.A. (1975). Effect of potassium nutrition on tomato plant growth and fruit development. *Plant and Soil* , 42, 395-412.

Cao, Y., Glass, A.D. & Crawford, N.M. (1993). Ammonium inhibition of Arabidopsis root growth can be reversed by potassium and by auxin resistance mutations aux1, axr1 and axr2. *Plant Physiol* 102, 983-989.

Chen, Y., Ma, J., Miller, A.J., Luo, B., Wang, M., Zhu, Z. & Ouwerkerk, P.B. (2016). OsCHX14 is involved in the K+ homeostasis in rice (Oryza sativa) flowers. *Plant Cell Physiol* , 57, 1530-2543.

Clarkson, D.T. & Hanson, J.B. (1980). The mineral nutrition of higher plants. *Annu Rev Plant Physiol* , 31, 239-298.

Ding, D., Zhang, L.F., Wang, H., Liu, Z.J., Zhang, Z.X. & Zheng, Y.L. (2009). Differential expression of miRNAs in response to salt stress in maize roots. *Annals of Botany* , 103, 29-38.

Gierth, M. & Maser, P. (2007). Potassium transporters in plants-involvement in K^+ acquisition, redistribution and homeostasis. *FEBS Lett* , 581, 2348-2356.

Han, Q.Q., Song, H.F., Yang, Y.N., Jiang, H. & Zhang, S. (2018). Transcriptional profiling reveals mechanisms of sexually dimorphic responses of PoPulus cathayana to potassium deficiency.*Physiologia Plantrum* , 162(3), 301-315.

Hu, B., Wang, W., Deng, K., Li, H., Zhang, Z., Zhang, L. & Chu, C. (2015). MicroRNA399 is involved in multiple nutrient starvation responses in rice. *Front Plant Sci* , 6, 188.

Kulcheski, F.R., Correa, R., Gomes, I.A., de Lima, J.C. & Margis, R. (2015). NPK macronutrients and microRNA homeostasis. *Front Plant Sci* , 6, 451.

Laegreid, M., Bockman, O.C. & Kaarstad, O. (1999). Agriculture, fertilizers and the environment. Norsk Hydro ASA, CABI Publishing.

Liu, H.H., Tian, X., Li, Y.J., Wu, C.A. & Zheng, C.C. (2008). Microarray-based analysis of stress-regulated microRNAs in*Arabidopsis thaliana* . *RNA* , 14, 836–843.

Lynn, K., Fernandez, A., Aida, M., Sedbrook, J., Tasaka, M., Masson, P. & Barton, M.K. (1999). The PINHEAD/ZWILLE gene acts pleiotropically in Arabidopsis development and has overlapping functions with the ARGONAUTE1 gene. *Development* , 126, 469-481.

Mahale, B.M., Fakrudin, B., Ghosh, S. & Krishnaraj, P.U. (2014). LNA mediated in situ hybridization of miR171 and miR397a in leaf and ambient root tissues revealed expressional homogeneity in response to shoot heat shock in Arabidopsis thaliana. *J.Plant Biochem. Biotechnol* , 23(1), 93-103.

Nam, Y.J., Tran, L.S., Kojima, M., Sakakibara, H., Nishiyama, R. & Shin, R. (2012). Regulatory roles of cytokinins and cytokinin signaling in response to potassium deficiency in Arabidopsis. *Plos One* , 7, e47797.

Schachtman, D.P. (2015). The role of ethylene in plant response to K^+ deficiency. *Front Plant Sci* , 6, 1153.

Qi, Y., Denli, A.M. & Hannon, G.J. (2005). Biochemical specialization within Arabidopsis RNA silencing pathways. *Mol Cell* , 19, 421-428.

Reinhart, B.J., Weinstein, E.G. & Rhoades, M.W. (2002). MicroRNAs in plants. *Genes &Development* , 16, 1616-1626.

Rigas, S., Ditengou, F.A., Ljung, K., Daras, G., Tietz, O., Palme, K. & Hatzopoulos, P. (2013). Root gravitropism and root hair development constitute coupled developmental responses regulated by auxin homeostasis in the Arabidopsis root apex. *New Phytol* , 197, 1130-1141.

Sato, A., Sato, Y., Fukao, Y., Fujiwara, M., Umezawa, T., Shinozaki, K., Hibi, T., Taniguchi, M., Miyake, H., Goto, D.B. & Uozumi, N. (2009). Threonine at position 306 of the KAT1 potassium channel is essential for channel activity and is a target site for ABA-activated SnRK2/OST1/SnRK2.6 protein kinase. *Biochem. J.* , 424, 439-448.

Shin, R. & Schachtman, D.P. (2004). Hydrogen peroxide mediates plant root response to nutrient deprivation. *Proc. Natl. Acad. Sci. USA* , 101, 8827-8832.

Song, W.J., Xue, R., Song, Y., Bi, Y., Liang, Z.H., Meng, L., Dong, C.X., Wang, C.D., Liu, G.L., Dong, J.X. & Zhang, Y.L. (2018). Differential response of First-Order Lateral Root Elongation to Low Potassium Involves Nitric Oxide in Two Tobacco Cultivars. *J Plant Growth Regul .*, 37, 114-127.

Tomari, Y. & Zamore, P.D. (2005). Perspective: machines for RNAi.*Genes & Dev* , 19, 517-529.

Vaucheret, H., Vazquez, F., Crete, P. & Bartel, D.P. (2004). The action of ARGONAUTE1 in the miRNA pathway and its regulation by the miRNA pathway are crucial for plant development. *Genes & Development* , 18, 1187-1197.

Vaucheret, H., Mallory, A.C. & Bartel, D.P. (2006). AGO1 homeostasis entails coexpression of MIR168 and AGO1 and preferential stabilization of miR168 by AGO1. *Mol Cell* , 22, 129-136.

Wang, Y. & Wu, W.H. (2017). Regulation of potassium transport and signaling in plants. *Current Opinion in Plant Biology* , 39, 123-128.

Weiler, E.W., Jourdan, P.S. & Conrad, W. (1981). Levels of indole-3-acetic acid in intact and decapitated coleoptiles as determined by a specific and decapitated coleoptiles as determined by a specific and highly sensitive solid-phase enzyme immunoassay. *Planta* , 153, 561-571.

Yang, Y.M., Xu, C.N., Wang, B.M. & Jia, J.Z. (2001). Effects of plant growth regulators on secondary wall thickening of cotton fibres.*Plant Growth Regul* , 35, 233-237.

Yan, K.S., Yan, S., Farooq, A., Han, A., Zeng, L. & Zhou, M.M. (2003). Structure and conserved RNA binding of the PAZ domain. *Nature* , 426, 468-474.

Zhao, X.M., Liu, Y., Liu, X. & Jiang, J. (2018). Comparative transcriptome profiling of two tomato genotypes in response to potassium-deficiency stress. *International Journal of Molecular Sciences* , 19, 2402.

Zhou, X., Wang, G., Sutoh, K., Zhu, J.K. & Zhang, W. (2008). Identification of cold-inducible microRNAs in plants by transcriptome analysis. *Biochem Biophys Acta* , 1779, 780–788.

Table 1. Relative miRNA expression of 10 DE miRNAs for comparison of the*35S:SlmiR-168a* versus WT groups and*35S:rSlAGO1* versus WT groups, in respect to by integrated analysis of mRNA-seq and miRNA-seq and Quantitative real-time PCR. * Asterisk indicates statistical significance of differential gene expression with p-value < 0.05 (t-test).

miR_name	Compared group	FC	Sig FC	Regulation	RT-PCR	mRNA	FC
stu-miR530_L-2R+2	35S:rSlAGO1/ JZ18	2.19	yes	up	1.96*	Solyc04g008110.3.1	0.20
						Solyc07g063510.3.1	0.45
ppe-miR858_1ss4GA	35S:rSlAGO1/ JZ18	2.33	yes	up	4.45*	Solyc05g006420.3.1	0.40
ath-miR171a-3p_L-3R+1	35S:rSlAGO1/ JZ18	inf	yes	up	inf*	Solyc08g069180.3.1	0.33
stu-miR8039_R+3_1ss4CT	35S:rSlAGO1/ JZ18	inf	yes	up	13.98*	Solyc12g056040.1.1	0.11
stu-miR384-5p_R+1	35S:rSlAGO1/ JZ18	inf	yes	up	10.45*	Solyc03g113890.1.1	0.09
						Solyc06g076850.3.1	0.43
PC-3p-276756_24	35S:rSlAGO1/ JZ18	inf	yes	up	2.23*	Solyc05g006420.3.1	0.40
PC-5p-289257_23	35S:rSlAGO1/ JZ18	inf	yes	up	7.62*	Solyc04g082420.3.1	0.37
PC-5p-66618_119	35S:rSlAGO1/ JZ18	4.29	yes	up	4.79*	Solyc08g066260.3.1	0.20
stu-MIR8006-p3_1ss8GA_1	35S:SlmiR-168a / JZ18	-inf	yes	down	-inf*	Solyc09g097780.2.1	2.59
stu-MIR8007b-p3_1ss22CT	35S:SlmiR-168a / JZ18	0.48	yes	down	-1.98*	Solyc09g064820.1.1	6.60

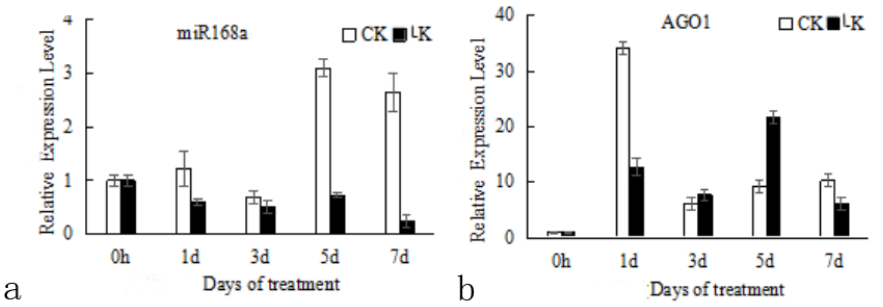

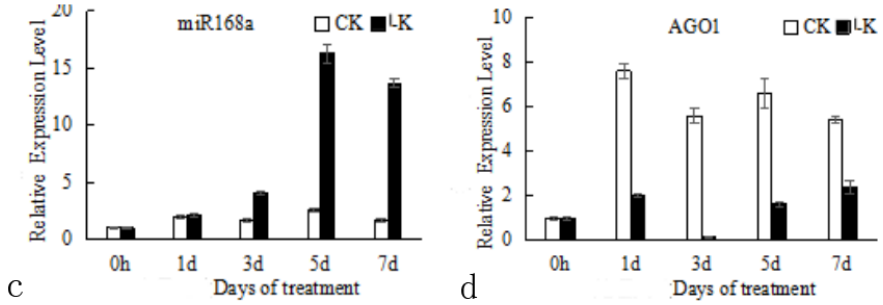

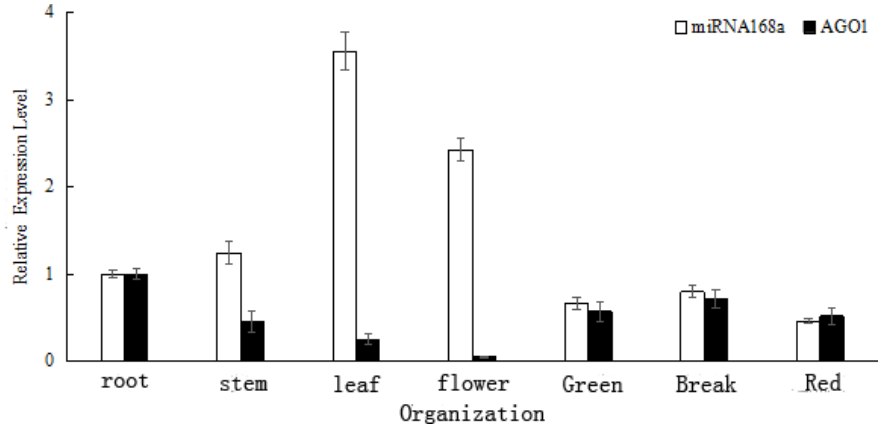

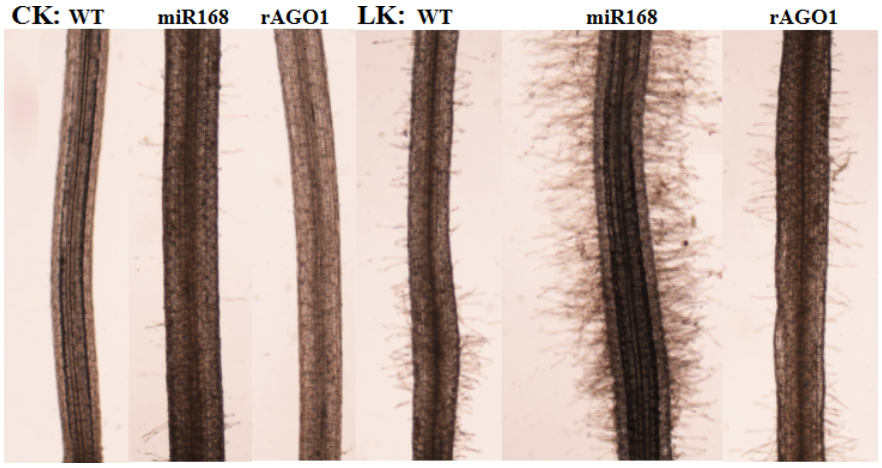

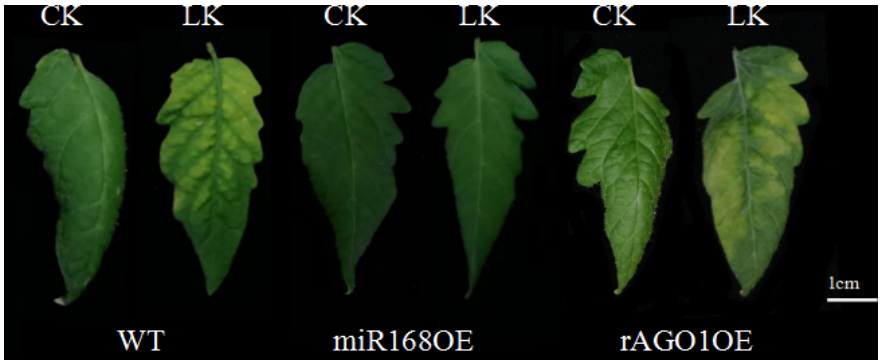

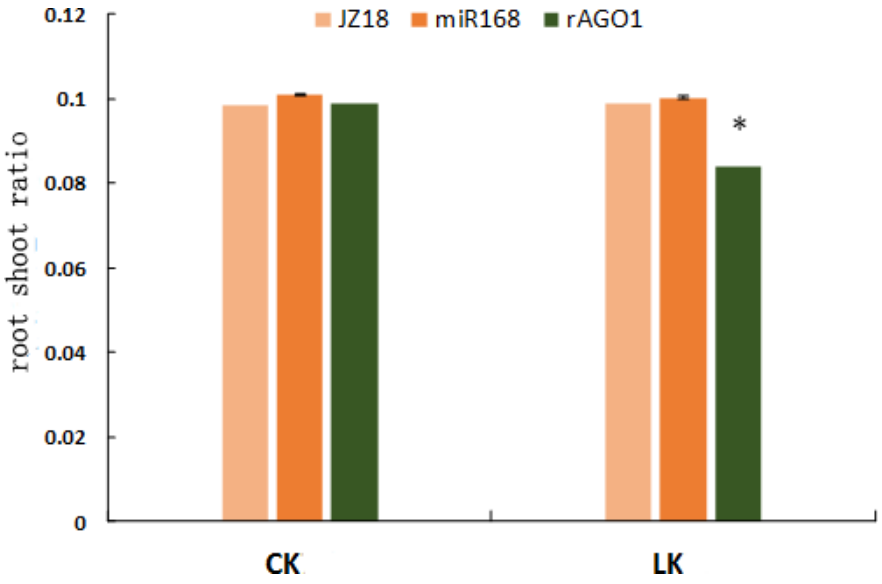

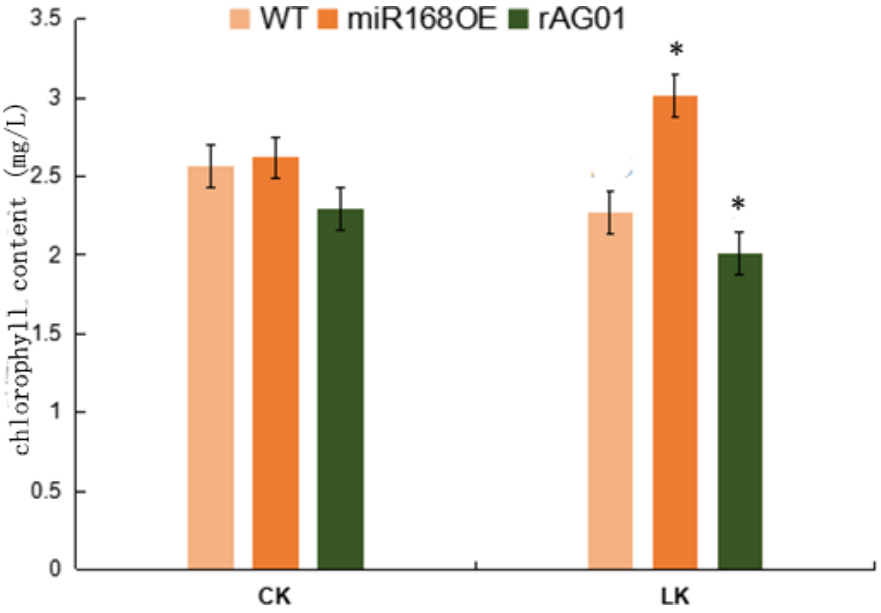

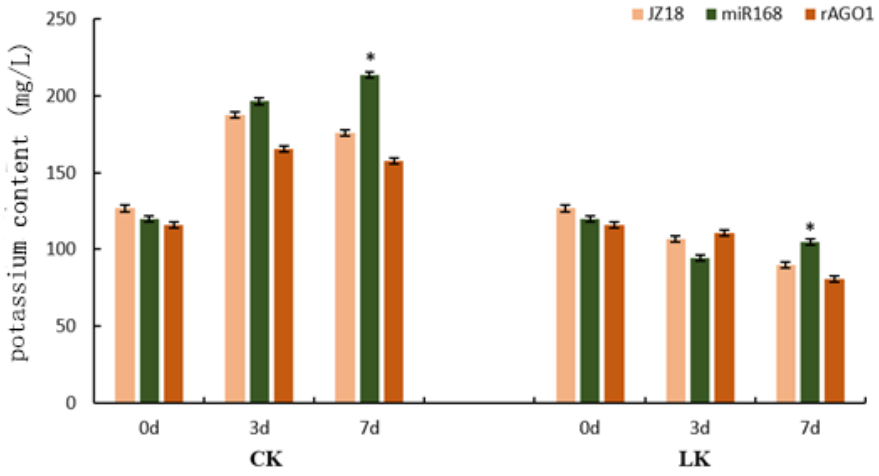

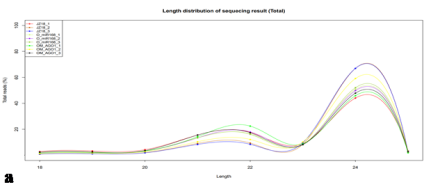

a

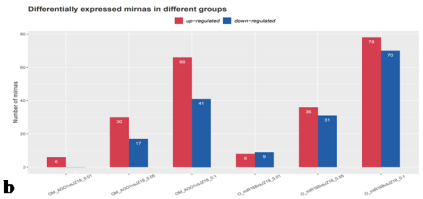

b